

BIOLOGY, STRUCTURE AND MECHANISM OF P-TYPE ATPases

Werner Kühlbrandt

P-type ATPases are ion pumps that carry out many fundamental processes in biology and medicine, ranging from the generation of membrane potential to muscle contraction and the removal of toxic ions from cells. Making use of the energy stored in ATP, they transport specific ions across the cell membrane against a concentration gradient. Recent X-ray structures and homology models of P-type pumps now provide a basis for understanding the molecular mechanism of ATP-driven ion transport.

MEMBRANE POTENTIAL

The charge difference (measured in mV) between the two surfaces of a biological membrane that arises from the different concentrations of ions such as H⁺, Na⁺ or K⁺ on either side. The Na⁺/K⁺-ATPase creates a membrane potential by using the energy stored in ATP to maintain a low concentration of Na⁺ and a high concentration of K⁺ in the cell, against a higher concentration of Na⁺ and a lower concentration of K⁺ on the outside.

In 1957, Jens Skou examined the effect of various cations on a homogenate of leg nerves from crabs that were caught on the shores of Denmark. The results led him to suggest that MEMBRANE POTENTIAL is generated by a K⁺-stimulated ATPase — now known as the Na⁺/K⁺-ATPase — that uses ATP to transport Na⁺ and K⁺ ions across the axonal membrane¹. Little did he know that he had just discovered the first P-type ATPase, and that this would win him the Nobel prize in chemistry 40 years later. In subsequent years, other ion pumps with similar characteristics were found in many different tissues and organisms. They include the sarcoplasmic-reticulum (SR) Ca²⁺-ATPase that helps to control the contraction of skeletal muscle², the gastric H⁺/K⁺-ATPase that acidifies the stomach, and the H⁺-ATPase that generates membrane potential in fungal and plant cells³. The biochemical characteristics that are common to these ion pumps are an acid-stable, phosphorylated Asp residue that forms during the pumping cycle (the phosphorylated (P) intermediate gives the family its name) and inhibition by orthovanadate, a transition-state analogue.

Almost 30 years ago⁴, it was established that the P-type ATPases undergo large conformational changes to translocate ions. Originally, two distinct conformations were called E1 and E2 (enzyme-1 and enzyme-2), with each having a different affinity for the nucleotide and the transported ions. Later, it became clear that the pumping cycle involves several further intermediate states⁵. Nevertheless, the E1/E2 nomenclature is almost

universally accepted and remains useful for identifying particular states. A summary of the catalytic cycle — or Post-Albers cycle — is shown in BOX 1. In their normal mode of action, P-type pumps use ATP to maintain an ion gradient across the cell membrane, but each step is reversible, so P-type ATPases can, in principle, use a membrane potential to produce ATP. For further information about the early literature on P-type ATPases, see REF. 6.

P-type pumps are a large, ubiquitous and varied family of membrane proteins that are involved in many transport processes in virtually all living organisms. A sequence alignment of four main representatives of the family (FIG. 1) shows a characteristic pattern of conserved residues, most notably the DKTGTLT sequence motif (in which D is the reversibly phosphorylated Asp). Another characteristic is the presence of 10 hydrophobic membrane-spanning helices (M1–M10; although some have only six or eight), and highly conserved cytoplasmic domains that are inserted between helices M2 and M3 and between M4 and M5. FIGURE 1 shows that 87 of the roughly 900 residues are invariant, with identical side chains or conservative substitutions in equivalent positions. As the four proteins that are compared in FIG. 1 are from widely different, unrelated organisms, there is no doubt that these conserved regions are structurally and functionally significant.

This article briefly reviews the distribution of P-type ATPases in biology, then presents a short overview of

Max-Planck Institut für
Biophysik, Marie-Curie-
Straße 13–15, 60439
Frankfurt am Main,
Germany.
e-mail:
Werner.Kuehlbrandt@mpi
bp-frankfurt.mpg.de
doi:10.1038/nrm1354

the different subfamilies and their ion specificities, before examining in some detail what the recent structures of entire enzymes or individual domains tell us about the fundamental mechanism of ATP-driven ion translocation.

P-type-ATPase genomics

In general, P-type-ATPase genes are more widespread and varied in eukaryotes than in bacteria and archaea. Only four P-type ATPases have been identified in *Escherichia coli*⁷. The thermophilic archaeon *Methanococcus jannaschii* has only one⁸, and certain parasitic bacteria seem to have none⁷. By contrast, the *Saccharomyces cerevisiae* genome has 16 P-type ATPases⁹, and no fewer than 45 have been identified in the *Arabidopsis thaliana* genome¹⁰, which points to their importance in vascular plants. Genome-wide searches in *Caenorhabditis elegans* and *Drosophila melanogaster* have turned up 21 and 15 genes, respectively¹¹. A corresponding analysis of P-type pumps in the human or mouse genome would be interesting, but has not yet been reported.

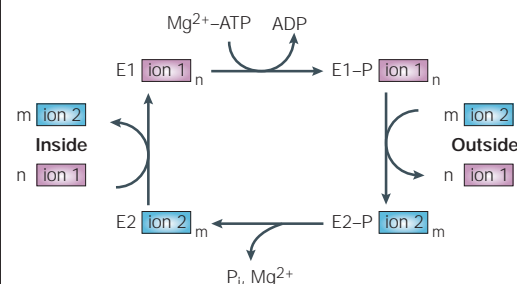
All P-type ATPases are multi-domain membrane proteins with molecular masses of 70–150 kDa. Both the carboxyl and amino termini are on the cytoplasmic side of the membrane, so they all have an even number of transmembrane segments. Based on sequence homology, the P-type-ATPase family can be divided into five branches (FIG. 2), which are referred to as types I–V. Within these branches, a total of 10 different subtypes or classes can be distinguished^{7,12}. Each subtype is specific for a particular substrate ion (FIG. 2). Functional studies might lead to further ramifications of the family tree, but it seems unlikely that entirely new, as yet undiscovered, branches will turn up in future genome searches.

Substrate specificity

Type-I ATPases. The simplest, and presumably most ancient, ion pumps are type-I pumps (FIG. 2). Type IA is a small class that contains bacterial ion pumps, with the *E. coli* Kdp K⁺-pump as the prototype. The Kdp pump is a complex of four different membrane proteins — that is, **KdpF**, **KdpA**, **KdpB** and **KdpC**. The 72-kDa KdpB subunit contains the catalytic core and ion-translocation site¹³ and, with only six membrane-spanning helices, the KdpB subunit is the smallest P-type ATPase.

Although most P-type ATPases translocate the small, 'hard' cations H⁺, Na⁺, K⁺, Ca²⁺ and Mg²⁺, the substrates of type-IB ATPases are 'soft'-transition-metal ions. Type-IB ATPases — for example, the bacterial metal-resistance proteins **CopA**¹⁴, **ZntA**¹⁵ and **CadA**¹⁶ — remove toxic ions such as Cu⁺, Ag⁺, Zn²⁺, Cd²⁺ or Pb²⁺ from the cell. The homeostasis of indispensable trace elements, such as Cu⁺ and Zn²⁺, is achieved by balancing the activity of these efflux pumps against ABC-type metal-uptake proteins^{16,17}. Unlike the type-IA ATPases, type-IB ATPases work as single-chain proteins and have eight membrane-spanning helices. Interestingly, they lack the last four helices in

Box 1 | The Post-Albers cycle



The general ion-translocation cycle of P-type ATPases (see figure) is based on the Post-Albers scheme for the Na⁺/K⁺-ATPase^{96,97}. In simple terms, ion 1 (X⁺ in FIG. 6) from the cell interior binds to a high-affinity site in the ATPase E1 state. Ion binding triggers phosphorylation of the enzyme by Mg²⁺-ATP, which leads to the phosphorylated E1-P state. The phosphorylated E2-P state then forms, which is unable to phosphorylate ADP, and this state has a reduced affinity for ion 1, which escapes to the outside. Ion 2 (Y⁺ in FIG. 6) binds from the outside and, on hydrolysis of the phosphorylated Asp, the enzyme releases ion 2 to the interior and re-binds ion 1. The enzyme is then ready to start another cycle. As a net result of this process, n ions of type 1 are expelled and m ions of type 2 are imported per molecule of ATP consumed — n and m are small integral numbers between 1 and 3. P_i, inorganic phosphate.

the consensus sequence (FIG. 1), but have an extra two helices at the amino-terminal end. Although most type-IB ATPases are bacterial, close homologues have been found in *S. cerevisiae*⁹, plants⁷ and animals¹⁸. Mutations in human Cu⁺-efflux pumps cause the rare, but lethal, hereditary Menkes and Wilson diseases. Because of their medical relevance, these pumps have received much attention since their discovery 10 years ago^{19,20–21}.

Type-IV and -V ATPases. The closest relatives of the type-I enzymes are types IV and V (FIG. 2). Type-IV ATPases have so far been found only in eukaryotes, in which they are involved in lipid transport and the maintenance of lipid-bilayer asymmetry. These 'lipid flippases' are thought to translocate phospholipids from the outer to the inner leaflet of, for example, red-blood-cell²² and *S. cerevisiae*²³ plasma membranes. The erythrocyte lipid flippase is a Mg²⁺-ATPase²⁴. Sequence comparisons show that they have the main features of the ion-translocating P-type ATPases⁷, including the ion-binding site in the membrane. In view of the close structural homology of the known P-type ATPases, it is difficult to imagine how the binding site at the centre of a 10-helix bundle can adapt to translocate both ions and phospholipids. Perhaps the lipid flippases are ion pumps that work in close association with ion-dependent, lipid-transport proteins such as the lipid-translocating ABC transporters²². Even more elusive than the lipid flippases are the type-V ATPases, which have

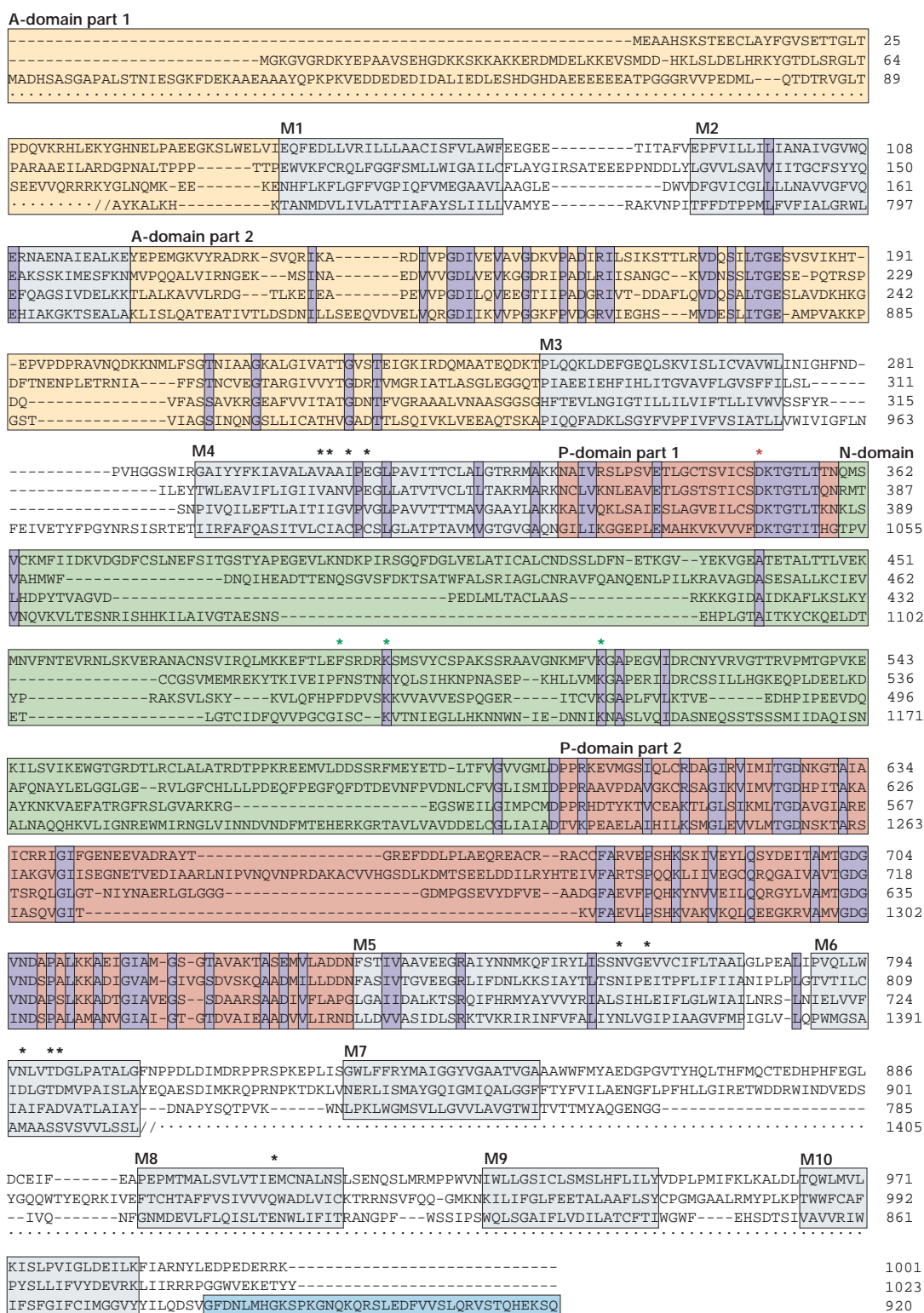


Figure 1 | **Conserved residues in P-type ATPases.** Sequence alignment of four representative P-type ATPases. From the top, the sequences of rabbit sarcoplasmic-reticulum Ca²⁺-ATPase, rat Na⁺/K⁺-ATPase, *Neurospora crassa* plasma-membrane H⁺-ATPase and the human Cu⁺-ATPase that is affected in Menkes disease are shown. The actuator (A)-domain is shaded in yellow, the phosphorylation (P)-domain in red, the nucleotide-binding (N)-domain in green, and the carboxy-terminal regulatory domain of the H⁺-ATPase in blue. The membrane-spanning helices M1–M10 are shaded grey. Identical residues and conservative substitutions are shaded purple. Coloured asterisks mark the phosphorylated aspartate (red), residues in the ion-binding site (black) and the nucleotide-binding site (green). For clarity, for the Cu⁺-ATPase, the large metal-binding, amino-terminal extension and the carboxy-terminal part beyond M6 are not included. Sequences were aligned using CLUSTAL 103.

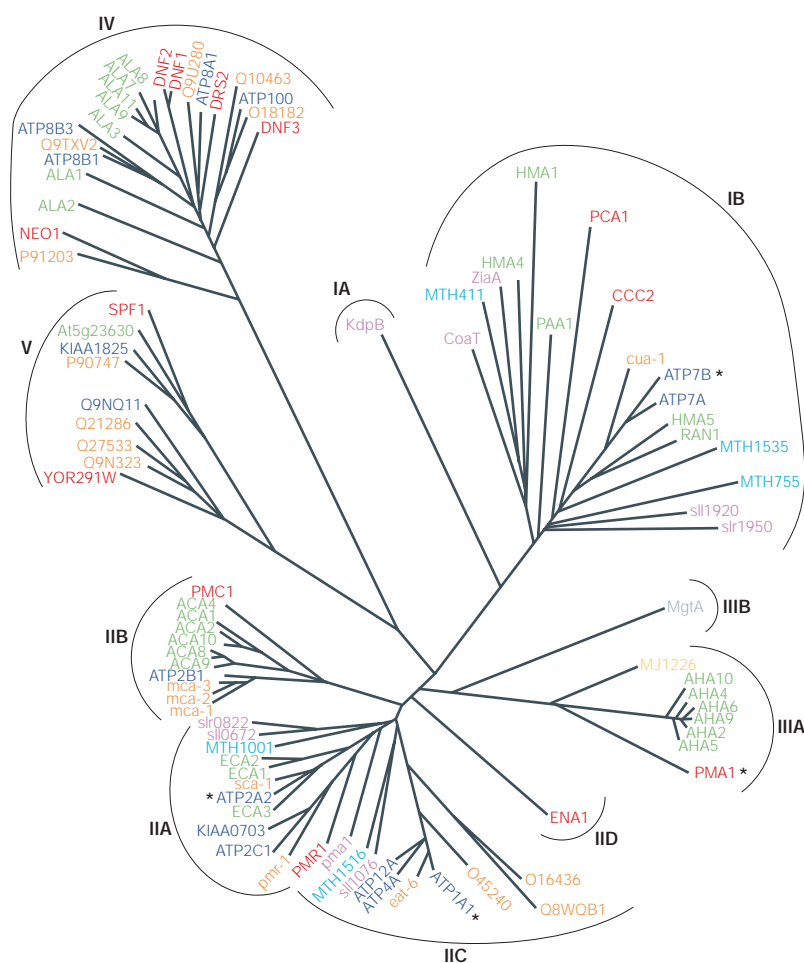


Figure 2 | Phylogenetic tree of the P-type-ATPase family. Subfamilies cluster according to their ion specificities: type IA, bacterial Kdp-like K^+ -ATPases; type IB, soft-transition-metal-translocating ATPases; type IIA, sarcoplasmic-reticulum (SR) Ca^{2+} -ATPases; type IIB, plasma-membrane Ca^{2+} -ATPases; type IIC, Na^+/K^+ -ATPases and H^+/K^+ -ATPases; type IID, eukaryotic Na^+ -ATPases; type IIIA, H^+ -ATPases; type IIIB, bacterial Mg^{2+} -ATPases; type IV, 'lipid flippases'; and type V, eukaryotic P-type ATPases of unknown substrate specificity. Representative gene products are colour coded by species: green, genes from *Arabidopsis thaliana*; orange, *Caenorhabditis elegans*; grey, *Escherichia coli*; dark blue, *Homo sapiens*; light blue, *Methanobacterium thermoautotrophicum*; yellow, *Methanococcus jannaschii*; purple, *Synechocystis* PCC6803; and red, *Saccharomyces cerevisiae*. Asterisks mark gene sequences of the closest relatives of those compared in FIG. 1 — that is, a mammalian SR Ca^{2+} -ATPase (ATP2A2; type IIA), a mammalian Na^+/K^+ -ATPase (ATP1A1; type IIC), a fungal H^+ -ATPase (PMA1; type IIIA), and a mammalian Cu^+ -ATPase (ATP7B; type IB). Classification is according to Axelsen and Palmgren⁷. This figure was kindly provided by Kristian Axelsen (Swiss Institute of Bioinformatics, Geneva). For clarity, gene names have not been italicized.

FXYP PROTEIN FAMILY

A small family of short, single-span membrane proteins that contain the FXYP sequence motif (in which X can be any amino acid). Most known FXYP proteins regulate the activity of Na^+/K^+ -ATPases in particular tissues. For example, the FXYP protein phospholemman regulates Na^+/K^+ -ATPases in heart and skeletal muscle, and the γ -subunit, another FXYP protein, regulates renal Na^+/K^+ -ATPase.

emerged recently as a separate class in eukaryotic genomes⁷. Their substrate specificities and biological roles are, as yet, unknown, but they are probably also ion pumps.

Type-II and -III ATPases. The most-investigated members of the P-type-ATPase family are those that create and maintain the membrane potential in animal and plant cells, which results from the often significantly different ion concentrations on either side of the membrane. This ion gradient is one of the indispensable attributes of living cells and powers the secondary

transport of sugars and amino acids, as well as other small molecules and ions. The main electrogenic P-type ATPases are all type-II or type-III ATPases (FIG. 2). Nearly everything we know about the structure, function and mechanism of the P-type-ATPase family comes from the main representatives of these branches.

Type-II ATPases are the most diverse. Type IIA comprises the SR Ca^{2+} -ATPase (for recent reviews, see REFS 25,26), whereas plasma-membrane Ca^{2+} -pumps belong to type IIB. The SR Ca^{2+} -ATPase has become the archetype of the P-type-ATPase family, because its atomic structure is the only one so far to have been determined experimentally^{27,28}. It pumps two Ca^{2+} ions out of muscle cells into the lumen of the SR per ATP, in exchange for two (REF. 29) or three (REF. 26) H^+ ions. The sudden release of Ca^{2+} back into the cell through Ca^{2+} channels results in muscle contraction³⁰. In plants, type-IIB Ca^{2+} -ATPases have numerous essential functions^{31,32}. The activity of type-IIA pumps in animal cells is regulated by phospholamban, whereas those of type IIB have carboxy- or amino-terminal, calmodulin-binding regulatory domains³³.

Type IIC includes the Na^+/K^+ -ATPases (for recent reviews, see REFS 34,35) and their close relatives, the gastric H^+/K^+ -ATPases^{36,37}. After the SR Ca^{2+} -ATPase, the Na^+/K^+ -ATPase is the next best-characterized P-type ATPase. This Na^+ -pump creates the membrane potential in mammalian cells by expelling three Na^+ ions in exchange for two imported K^+ ions per cycle. In active tissues such as kidney, it is estimated to consume ~30% of the cellular ATP³⁵. Both the Na^+/K^+ -ATPase and the H^+/K^+ -ATPase are important drug targets in humans³⁸. The Na^+/K^+ -ATPase is the target of digitalis glycosides, which have been used for centuries in the treatment of heart conditions. The H^+/K^+ -ATPase is inhibited by omeprazole³⁹, a potent anti-ulcer drug that prevents the excess production of stomach acid.

The type-IIC ATPases are hetero-oligomers. The catalytic α -subunit has all the characteristics of P-type ATPases, including the M1–M10 helices, whereas the β -subunit is a heavily glycosylated, single-membrane-spanning, ~55-kDa membrane protein. The β -subunit seems to be essential for assembly and membrane insertion⁴⁰, although some of the α - and β -subunits identified in the *C. elegans* and *D. melanogaster* genomes might not assemble into hetero-oligomers¹¹. Renal Na^+/K^+ -ATPases have additional regulatory γ -subunits⁴¹, which are members of the FXYP PROTEIN FAMILY⁴². The type-IID ATPases are eukaryotic Na^+ -ATPases.

Type-III A ATPases are H^+ -pumps that are found almost exclusively in the plasma membranes of plants and fungi, with only one exception so far (that is, the putative H^+ -pump of *M. jannaschii*⁴³). These H^+ -ATPases are able to maintain an intracellular pH of ~6.6 against an extracellular pH of 3.5 (REF. 44), which corresponds to a membrane potential of -180 mV. Interestingly, the membrane potential in plants and fungi is a proton potential, whereas the membrane potential in animal cells results from an Na^+/K^+ gradient³⁵. Accordingly, the Na^+/K^+ -ATPases that maintain this Na^+/K^+ gradient are absent in the plant kingdom, in which their place is

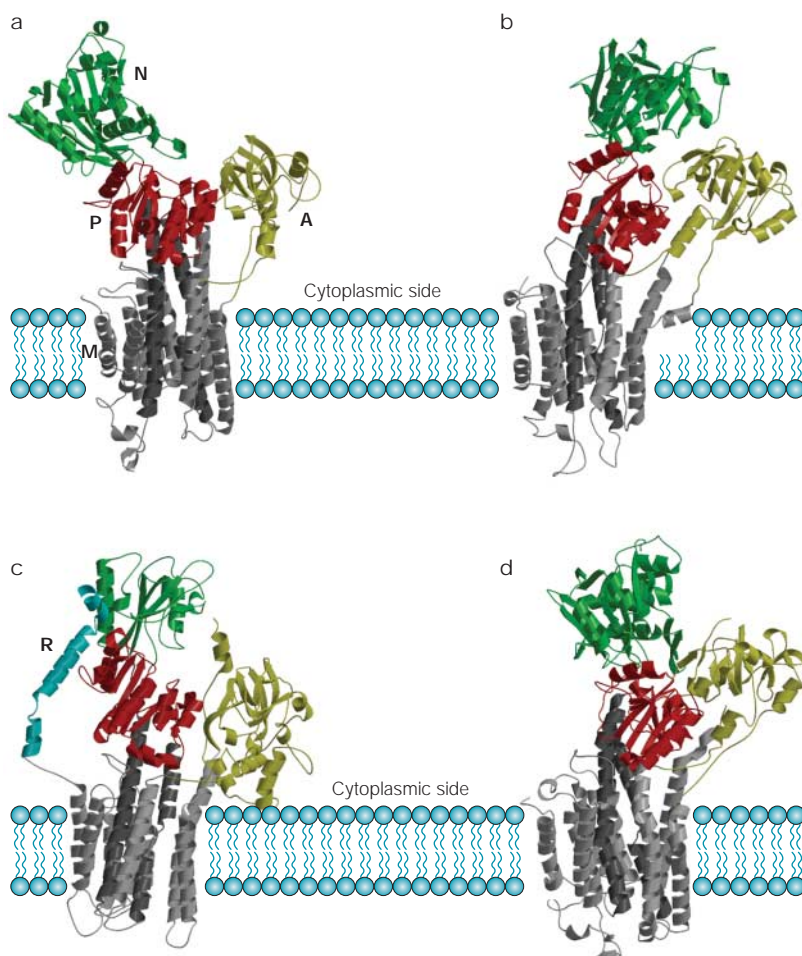


Figure 3 | P-type-ATPase structures and models. **a** | Sarcoplasmic-reticulum (SR) Ca^{2+} -ATPase in the E1 state²⁷. **b** | SR Ca^{2+} -ATPase in the thapsigargin-inhibited E2 state²⁸. **c** | A homology model of the *Neurospora crassa* plasma-membrane H^{+} -ATPase in the E1 state⁵⁵. **d** | A homology model of the duck-salt-gland $\text{Na}^{+}/\text{K}^{+}$ -ATPase⁴⁹ in the vanadate-inhibited, phosphorylated E2 state (E2-P). The phosphorylation (P)-domain is shown in red, the nucleotide-binding (N)-domain in green, the actuator (A)-domain in yellow, the membrane (M)-domain in grey, and the carboxy-terminal regulatory (R)-domain of the *N. crassa* plasma-membrane H^{+} -ATPase in blue. The two long helices, M4 and M5, that connect the ion-binding site to the P-domain are shown in a darker shade of grey. Coordinates for the structure shown in part **d** were kindly provided by David Stokes (New York University Medical School, USA).

taken by the type-III H^{+} -pumps. Unlike the type-II enzymes, the H^{+} -ATPases have autoinhibitory, carboxy-terminal extensions. The closest relatives of the type-III A ATPases are the type-IIIB ATPases, which are a small class of bacterial Mg^{2+} -pumps.

P-type-ATPase structure

Structural studies of P-type ATPases go back more than twenty years. Two-dimensional crystals of a renal $\text{Na}^{+}/\text{K}^{+}$ -ATPase were first obtained by incubating kidney-cell membranes with vanadate⁴⁵, a transition-state analogue that traps P-type ATPases in the phosphorylated E2 state (E2-P). Similar experiments produced tubular crystals of the SR Ca^{2+} -ATPase⁴⁶ and two-dimensional arrays of the gastric-mucosa $\text{H}^{+}/\text{K}^{+}$ -ATPase⁴⁷. Electron-microscopy (EM) studies on such crystals have provided three-dimensional (3D) maps at progressively

higher resolutions, most recently at 6 Å for the SR Ca^{2+} -ATPase⁴⁸ and at 11 Å for the $\text{Na}^{+}/\text{K}^{+}$ -ATPase⁴⁹ (both in the E2-P state). A 3D map of the *Neurospora crassa* H^{+} -ATPase in the E1 state has been determined to a resolution of 8 Å by electron cryo-microscopy⁵⁰, and projection maps at 8-Å resolution have been obtained for an *A. thaliana* H^{+} -ATPase that was expressed in *S. cerevisiae*⁵¹. Finally, X-ray crystallography yielded a 2.6-Å structure of the SR Ca^{2+} -ATPase in the E1 state, with two Ca^{2+} ions bound to it²⁷ (FIG. 3a).

The X-ray crystal structure of the Ca^{2+} -ATPase²⁷ has been a turning point in the recent study of P-type ATPases. Although the predicted 10 transmembrane segments had been seen before in EM maps of this Ca^{2+} -ATPase⁵² and the *N. crassa* H^{+} -ATPase⁵⁰, details of the catalytic sites in the cytoplasmic domains and the ion-binding site in the membrane had to await a higher resolution structure. The most surprising discovery was the long distance between the nucleotide-binding and phosphorylation sites (25 Å), and the even longer distance between the phosphorylation site and the ion-binding site in the membrane (~45 Å). The first comparisons of this structure with EM maps of the same protein in the vanadate-inhibited E2-P conformation^{27,48} indicated that pronounced, rigid-body rearrangements of the cytoplasmic domains occur, and this was confirmed by the 3.1-Å structure of the Ca^{2+} -ATPase in the thapsigargin-stabilized E2 state²⁸ (FIG. 3b). A recent 1.2-Å structure of a phosphorylation (P)-domain analogue⁵³ and NMR structures of the $\text{Na}^{+}/\text{K}^{+}$ -ATPase nucleotide-binding (N)-domain with and without bound ATP⁵⁴ have helped us to further understand the molecular mechanism of P-type ATPases. For a brief discussion of the methods used to determine these structures, see BOX 2.

Model building

In the absence of other high-resolution structures, the SR Ca^{2+} -ATPase in the E1 state²⁷ has proved to be an excellent template for homology modelling of different states, and of related P-type ATPases (BOX 3). A homology model of the *N. crassa* H^{+} -ATPase⁵⁵ in the E1 state⁵⁰ (FIG. 3c) highlighted a significant difference in the position of the N-domain. A model of the duck-salt-gland $\text{Na}^{+}/\text{K}^{+}$ -ATPase in the vanadate-inhibited E2-P state⁴⁹ (FIG. 3d) was obtained in a similar way.

Other published models of the renal $\text{Na}^{+}/\text{K}^{+}$ -ATPase³⁴ and the *A. thaliana* plasma-membrane H^{+} -pump³² were not fitted to experimentally determined EM maps and are therefore largely identical to the E1 target structure. A detailed homology model of the $\text{Na}^{+}/\text{K}^{+}$ -ATPase membrane (M)-domain⁵⁶ has postulated the location of the three Na^{+} - and two K^{+} -binding sites.

The four principal domains

The SR Ca^{2+} -ATPase consists of four well-defined protein domains (FIG. 3a). According to their function or position, they are referred to as the P-domain, the N-domain, the actuator (A)-domain and the M-domain. It is clear from the sequence comparison

Box 2 | Structural methods in molecular cell biology

X-ray crystallography

This method is unrivalled for determining protein structures at the highest level of detail, such as a 1.2-Å-resolution structure of a P-type-ATPase phosphorylation-domain analogue⁵³ (please refer to the main text for further details). It is dependent on being able to obtain highly ordered crystals, which are often difficult to grow for membrane proteins. However, for soluble proteins or heterologously expressed protein domains, X-ray crystallography is now routine. The structures of small proteins can be determined in weeks or even days by semi-automatic methods, especially if the methionine residues in the protein are replaced by selenomethionine for accurate phase determination.

NMR spectroscopy

This method is the second-most popular method for determining protein structures. The structures are generally less accurate than those determined by X-ray crystallography, although particular chemical groups — such as the ATP in the NMR structure of the Na⁺/K⁺-ATPase nucleotide-binding domain⁵⁴ — can be more clearly defined. An important advantage is that the protein does not have to be crystallized. However, solution NMR requires a high concentration of protein that is labelled with isotopes (usually ¹³C, ¹⁵N or ²H). NMR spectroscopy works best with proteins of up to ~30 kDa, which excludes most membrane proteins, but methods for tackling larger structures are being developed.

Electron cryo-microscopy

Electron cryo-microscopy is the method of choice for determining the structures of large, multi-protein assemblies, and of membrane proteins that do not easily form crystals for X-ray crystallography (including the *Neurospora crassa* H⁺-ATPase⁵⁰). Electron cryo-microscopy of membrane proteins requires two-dimensional crystals, which are usually easier to grow than three-dimensional crystals, and can produce structures at near-atomic resolution — as was the case for bacteriorhodopsin⁹⁸, the plant light-harvesting complex⁹⁹ and the nicotinic acetylcholine receptor¹⁰⁰. Large complexes, such as H⁺-ATPase hexamers⁸⁹, are studied by electron-image processing of non-crystalline proteins that have been rapidly frozen in a thin layer of buffer. Resolutions of ~10–20 Å can be obtained, although higher resolutions have been achieved by combining data from 10,000 or more particles.

(FIG. 1) that these four principal domains are conserved throughout the P-type ATPase family. Deletions and insertions are mainly restricted to the extracytoplasmic loops, or to stretches that connect conserved elements of secondary structure in the cytoplasmic domains. Residues that are required for the core enzymatic functions are invariant (FIG. 4).

The phosphorylation domain. The P-domain is the catalytic core of the SR Ca²⁺-ATPase, as it contains the DKTGTLT signature sequence (FIG. 1). It is roughly spherical and has a ROSSMANN FOLD with a central seven-stranded β-sheet flanked by α-helices, including the cytoplasmic end of M5. Its sequence is the most highly conserved of the four principal domains, with 39% of residues being identical between the *N. crassa* H⁺-ATPase and the SR Ca²⁺-ATPase, and few insertions or deletions (FIG. 1). Apart from the reversibly phosphorylated Asp (Asp351 in the SR Ca²⁺-ATPase) and the hinges that link the P-domain to the N-domain, most of the invariant residues are found in the central β-sheet (FIG. 4), which has no direct role in the enzyme mechanism but must be important for folding.

The P-domain is homologous to a class of bacterial enzymes⁵⁷ that use a corresponding, reversibly phosphorylated Asp as a reaction intermediate. Recently, the structure of the transition state of one of these enzymes — β-phosphoglucomutase (β-PGM) — was determined at 1.2-Å resolution, which remarkably showed the Asp in the process of being phosphorylated⁵³. The central β-sheet of the Rossmann fold of β-PGM and the position of the phosphorylated Asp superimpose exactly on the P-domain structure (FIG. 5a). The β-PGM structure shows how the Mg²⁺ ion compensates the charge, and coordinates the precise geometry, of this Asp (Asp8

in β-PGM), and therefore enables phosphoryl transfer to take place. Presumably, the reaction mechanism and the role of the bound Mg²⁺ ion is similar in the P-type ATPases.

The nucleotide-binding domain. The N-domain is a large insert in the P-domain (FIG. 1), to which it is linked by a strongly conserved hinge of two antiparallel peptide strands. Its central structural element is a β-sheet of seven strands in the SR Ca²⁺-ATPase. A conserved sequence motif, which includes Lys515, defines the nucleotide-binding site²⁷. The size and sequence of the N-domain varies more than that of the other cytoplasmic domains. In the *N. crassa* H⁺-ATPase, it is 40% smaller than in the SR Ca²⁺-ATPase (FIG. 3a,c) and only 20% of the residues — mainly those in the immediate environment of the nucleotide-binding site — are conserved (FIG. 1).

The structure of a rat Na⁺/K⁺-ATPase N-domain that was expressed in *E. coli* was determined by solution NMR⁵⁴. As expected, it has the same overall fold as the SR-Ca²⁺-ATPase N-domain. The central, twisted antiparallel β-sheet has six rather than seven (or eight as has been predicted for the Na⁺/K⁺-ATPase³⁵) strands, but the flanking helices are in the same positions as in the SR Ca²⁺-ATPase. Differences are mostly confined to the loops that join the β-strands and helices. One characteristic of the Na⁺/K⁺-ATPase N-domain is a hydrophobic cluster of Phe residues that replace acidic residues in the SR Ca²⁺-ATPase. Other inserts might be important for regulation, such as the phospholamban-interaction site in the SR Ca²⁺-ATPase⁵⁸.

This structure⁵⁴ shows the position and orientation of ATP in the nucleotide-binding site more clearly than the X-ray structure²⁷ (FIG. 5b). Surprisingly, only the

ROSSMANN FOLD

A common structural motif that is found in the nucleotide-binding domains of many proteins. The typical Rossmann fold (named after the eminent protein crystallographer Michael Rossmann) consists of two structurally similar halves, each with three β-strands and two α-helices. The two halves are connected by a linking helix, and form a compact, globular α/β domain with a central, six-stranded parallel β-sheet.

Box 3 | Homology modelling

Homology modelling of protein structures is based on the observation that proteins with homologous sequences also have similar three-dimensional structures¹⁰¹. Therefore, the unknown structure of a protein can be modelled on the experimentally determined structure of a related protein. Key to a reliable model is the sequence alignment. Aligning a large number of sequences — as in the case of the P-type ATPases — by standard procedures such as BLAST¹⁰² or CLUSTAL¹⁰³ works well, but manual adjustment of the aligned sequences might be necessary to take other evidence, such as biochemical crosslinking, into account. A computer program (for example, MODELLER¹⁰⁴) then calculates a model in which the coordinates of conserved residues are taken from the target structure, using the most-probable bond lengths and bond angles. Weakly homologous regions, which are frequently found in surface loops, are approximated on the basis of similar loops in known protein structures, and are therefore less reliable than the highly conserved regions. The amino-acid side chains in these regions are placed in their preferred orientation, and finally the model is optimized using molecular dynamics and probability-density functions. The homology model of the *Neurospora crassa* H⁺-ATPase⁵⁵ (FIG. 3c) was generated in this way on the basis of the X-ray structure of the sarcoplasmic-reticulum Ca²⁺-ATPase in the E1 state²⁷ (FIG. 3a).

adenosine base of ATP sits in the binding pocket, with Phe475 providing a platform for hydrophobic stacking, whereas the triphosphate group protrudes into the solvent. This would explain how the γ -phosphate reaches the P-domain Asp that will be phosphorylated.

The thapsigargin-inhibited E2 form of the SR Ca²⁺-ATPase (FIG. 3b), and the vanadate-inhibited E2–P form of the Na⁺/K⁺-ATPase (FIG. 3d) show similar positions for their N-domains. In both cases, this domain seems to interact with the A- and P-domains. However, in the two available E1 structures, the N-domain assumes very different positions. In the H⁺-ATPase model (FIG. 3c), it is rotated by 73° towards the phosphorylation site and, in both E1 structures, there is no contact with the A-domain. Apparently, its position depends primarily on intermolecular crystal contacts. In the free enzyme, it probably oscillates by tethered Brownian motion on its hinge to deliver bound ATP to the phosphorylation site^{26,48,55}.

The actuator domain. The amino-terminal A-domain is the smallest cytoplasmic domain of the SR Ca²⁺-ATPase. Its sequence is almost as highly conserved as that of the P-domain (FIG. 1). It is therefore safe to assume that the 3D structure of the A-domain will be similar in all P-type ATPases. Like the P-domain, it is discontinuous and is divided into two unequal sections by the hairpin of helices M1 and M2. The larger second section has a β -sheet jelly-roll fold and contains a long stretch of highly conserved residues, including a loop that contains the invariant TGE sequence motif.

Unlike the other three SR-Ca²⁺-ATPase domains, the A-domain does not contain a distinct ion- or cofactor-binding site, and its role in the catalytic cycle was therefore not immediately obvious. Cleavage of the TGE loop⁵⁹ (see below) indicated that it contacts the phosphorylation site closely during the ion-pumping cycle, but in the Ca²⁺-ATPase E1 structure it is ~30 Å away from the phosphorylatable Asp. In the E2 structure of the SR Ca²⁺-ATPase²⁸, this distance is only ~11 Å, owing to a rotation of the A-domain around an axis that is

roughly perpendicular to the membrane. The EM-based model of the vanadate-inhibited E2–P state⁴⁸ puts the TGE loop into contact with the phosphorylation site, which confirms its prominent role in the molecular mechanism (FIG. 6).

Some P-type ATPases have amino-terminal extensions that are fused to the A-domain. In the fungal H⁺-ATPases, these extensions are 70–100 residues long and contain several clusters of acidic side chains. The soft-transition-metal ATPases have even longer extensions of up to ~750 residues that contain two to six repeats of a heavy-metal-binding motif, plus two extra membrane-spanning helices. The structures of two metal-binding subdomains have been determined by solution NMR^{60,61}. Conceivably, the metal-binding sites in the soft-transition-metal pumps, and the clusters of acidic residues in the H⁺-pumps, interact with the corresponding ions, and this might affect the mobility of the A-domain. However, a role for the amino-terminal extensions in substrate sensing and the regulation of ATPase activity has yet to be demonstrated.

The membrane domain. The M-domain consists of the 10 membrane-spanning helices (M1–M10) that surround the ion-binding sites in the membrane (FIG. 5c), as well as the short connecting loops on the outer membrane surface. With 405 residues in the SR Ca²⁺-ATPase and 351 in the *N. crassa* H⁺-ATPase, it is the largest of the four principal domains. Even though M-domains have a low degree of sequence homology (18%), their overall structures seem to be very similar. Evidently the structures of P-type ATPases are more highly conserved than their sequences, as has been found for other protein families with low sequence homology⁶². M1, M3, M7, M9 and M10, show virtually no homology between the various types of P-type ATPase. Apparently, there is little evolutionary pressure to preserve residues that are functionally unimportant, in particular those that face the lipid bilayer, as in the family of G-protein-coupled receptors⁶³.

Like the N-domain, the M-domain is directly linked to the catalytic core of the P-domain through the long M4 and M5 helices. The ion-translocation site in the SR Ca²⁺-ATPase is defined by two Ca²⁺ ions that are coordinated by polar and ionic side chains of M4, M5, M6 and M8 (REF. 27). A detailed view of the side chains that contribute to the binding site in the presence and absence of Ca²⁺ is shown in FIG. 5c. The acidic side chains of Asp800 in M6 and Glu908 in M8 have key roles in Ca²⁺ coordination. The corresponding side chains — Asp730 and Glu805 — are conserved in the *N. crassa* H⁺-ATPase. Asp684 in the *A. thaliana* H⁺-ATPase, which is equivalent to Asp730 in the *N. crassa* H⁺-ATPase, is crucial for proton translocation^{64,65}, but this does not seem to be the case for the equivalent of Glu805. Apart from these two residues, the main-chain carbonyls of Val304, Ala305 and Ile307 in M4 of the SR Ca²⁺-ATPase also participate in Ca²⁺ binding. The corresponding amino-acid side chains in the *N. crassa* H⁺-ATPase are different, but because Pro335 and Pro339 (Pro308 and Pro312 in the SR Ca²⁺-ATPase) are conserved, the main-chain carbonyls of the corresponding

residues might equally be available for ion binding. Other polar residues in M5 that are close to the SR- Ca^{2+} -ATPase ion-binding site are Tyr763 and Asn768, which are replaced by Tyr694 and Ser699 in the *N. crassa* H^{+} -ATPase.

In contrast to the SR Ca^{2+} -ATPase, the ion-binding site of the *N. crassa* H^{+} -ATPase includes Arg695 and His701 in M5. Both are completely conserved in fungal plasma-membrane H^{+} -ATPases. In plant H^{+} -pumps, Arg695 is replaced by Ala, whereas His701 is replaced by Arg. An Arg residue on M5 therefore seems to be important for ion translocation by the H^{+} -ATPase family. It has been proposed that this Arg substitutes for Ca^{2+} in one of the ion-binding sites and forms an ion bridge with an acidic side chain. This leaves the second site unoccupied⁶⁶, which could accommodate a hydronium (H_3O^+) ion. However, the number of protons that are translocated per reaction cycle, and whether they are transported as H_3O^+ , remains a matter of debate.

Whereas the P-, N- and A-domains move essentially as rigid bodies, the two X-ray structures of the SR Ca^{2+} -ATPase^{27,28} show significant differences in the arrangement of helices in the M-domain. The helix movements are centred on M5, which forms the backbone of the structure and, along with M4 and M6, seems to be mainly responsible for mechanically coupling events at the ion-binding site to those at the phosphorylation site, which is some 40-Å away. A comparison of the E2 and E1 states shows that the bending of M5 is associated with a 30° tilt of the P-domain, and that the lower end of M5 remains fixed against the M7–M10 bundle. It seems that a twist of M6 makes the side chains that contribute to the ion-binding site rotate sideways by ~90°, and an apparent piston movement of M4 displaces the main-chain and side-chain Ca^{2+} ligands in this helix upwards by 4–5 Å. The combined effect of these movements would be to create two Ca^{2+} -chelating sites in the M-domain (FIG. 5c), which apparently results in a 1,000-fold increase in binding affinity in the E1 state²⁶.

A common molecular mechanism

Most invariant residues in the SR- Ca^{2+} -ATPase structure are located in the three cytoplasmic domains, whereas only a few are found in the membrane-spanning helices (FIG. 4). This reflects different roles of the cytoplasmic and membrane domains in the translocation mechanism. The reactions of ATP binding, phosphoryl transfer and hydrolysis, and the mechanical transduction of the energy released in this process to the ion-binding site, are essentially the same in all P-type ATPases. Correspondingly, the structures of the functional sites in the P-, N- and A-domains that carry out these reactions are unchanged. The ion-binding sites in the M-domain, on the other hand, must be precisely tailored to accommodate different numbers of ions with different charges, radii and coordination geometries. This would explain why few, if any, of the functional residues in the M-domain are conserved. However, its overall 3D structure is maintained, as seen most clearly in the comparison of the SR- Ca^{2+} -ATPase E1 structure (FIG. 3a) and the

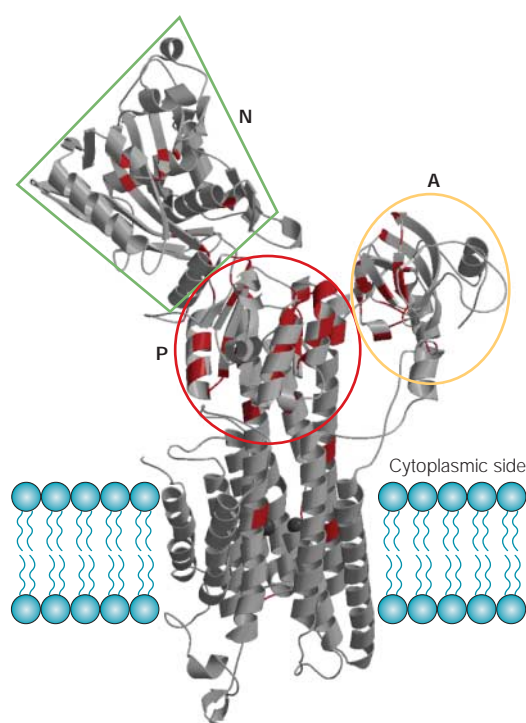


Figure 4 | Conserved residues in the sarcoplasmic-reticulum Ca^{2+} -ATPase. The position of invariant residues and conservative substitutions (highlighted in purple in the four aligned sequences of FIG. 1) are shown here in red on the structure of the sarcoplasmic-reticulum Ca^{2+} -ATPase. The orientation shown was chosen to highlight the conserved sites with minimal overlap. Most invariant residues are found in the phosphorylation (P)- and actuator (A)-domains, fewer in the nucleotide-binding (N)-domain, and hardly any in the 10 membrane-spanning helices. Their uneven distribution reflects a high degree of structural preservation in the domains that are involved in ATP binding, phosphoryl transfer and hydrolysis, which indicates that the molecular mechanisms are highly conserved. A high proportion of invariant residues in the cytoplasmic part are buried, many of them in β -sheets or the inward-facing sides of α -helices. Their primary role might be to ensure that the precise geometry of functionally important sites is maintained. Sequence conservation in the membrane domain is low because of the adaptation of the ion-binding site to different substrate ions, and because there is little evolutionary pressure to conserve hydrophobic, functionally unimportant residues that face the lipid bilayer⁶³. Nevertheless, the structure of this domain is highly conserved.

N. crassa H^{+} -ATPase model (FIG. 3c). This division of labour between the cytoplasmic and membrane domains helps us to understand how the P-type ATPases work.

It is too early to say whether the large movements of the three cytoplasmic domains and the internal rearrangements of the M-domain are, in fact, necessary for ATP hydrolysis and ion translocation, or to what extent they are exaggerated by intermolecular contacts in the various crystal structures of an inherently flexible multi-domain protein. However, assuming that the available structures and models do indeed represent actual reaction-cycle intermediates, we can now begin to reconstruct the sequence of molecular events in the

ion-pumping cycle as a dynamic, 3D puzzle. Although the emerging picture is not complete, the principles of the molecular mechanisms of ATP-driven ion translocation in P-type ATPases are finally becoming clear. An outline of the reaction cycle, as it appears from the available evidence, is shown in FIG. 6.

At the start of the cycle, ion 1 (X^+ in FIG. 6) reaches the high-affinity binding site(s) in the E1 state through an access channel from the cytoplasm and displaces ion 2 (Y^+ in FIG. 6), which presumably leaves through the same channel. The coordination of the incoming cations by the acidic and polar side chains provides the energy that pulls helices M4, M5 and M6, and the P-domain, into the E1 conformation.

Mg^{2+} -ATP binding to the N-domain seems to cause a slight change in the β -strands, as was observed in the

NMR structure⁵⁴, which might help the N-domain to approach to the P-domain more closely. The presumed oscillating motion of the N-domain ensures that the γ -phosphate of ATP occasionally reaches down to the phosphorylation site in the transition to the E1-P state (FIG. 6). The E1-P state is characterized by the occlusion of ion 1 in the binding site, which is then not accessible from either membrane surface. The exact positions of the cytoplasmic domains in the E1-P state are not yet known, but recent proteolytic-cleavage experiments indicate that it resembles the E1 state more than E2 and E2-P⁶⁷. It is probable that the phosphorylation reaction proceeds by the same mechanism as in β -PGM⁵³ (FIG. 5a,b), and that the bound Mg^{2+} ion facilitates the nucleophilic attack of the Asp in the P-domain on the γ -phosphate of ATP by reducing electrostatic repulsion

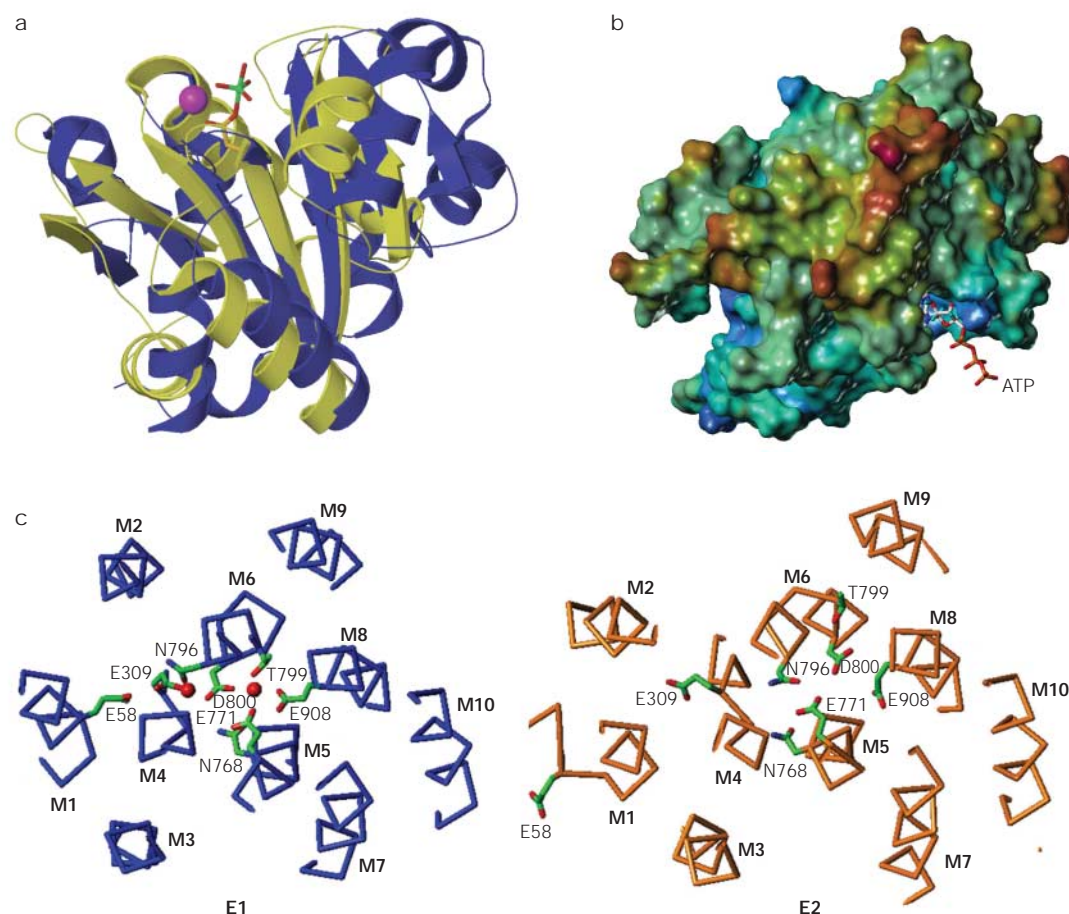


Figure 5 | Detailed views of P-type-ATPase domains and a domain homologue. **a** | Superposition of the sarcoplasmic-reticulum (SR)- Ca^{2+} -ATPase phosphorylation (P)-domain²⁷ (dark blue) and β -phosphoglucomutase⁵³ (β -PGM; yellow). Asp8 in β -PGM corresponds to Asp351 in the SR Ca^{2+} -ATPase, and the β -PGM structure shows Asp8 in the process of being phosphorylated. The Mg^{2+} ion (purple) next to the γ -phosphate (shown in a stick representation) stabilizes the pentacovalent transition state. The reaction mechanism of the P-type ATPases is probably similar. Residues 17 to 84 in the β -PGM structure, which correspond to an insert at the position of the SR- Ca^{2+} -ATPase nucleotide-binding (N)-domain, have been removed for clarity. **b** | NMR structure of the N-domain of rat Na^+/K^+ -ATPase with ATP bound⁵⁴. ATP binds with the adenosine base buried in the binding pocket and the triphosphate protruding beyond the surface to reach the Asp in the P-domain. A surface-potential representation of the domain is shown using Kollman charges (red, acidic; blue, basic). **c** | The ion-binding site in the membrane (M)-domain of the SR Ca^{2+} -ATPase in the E1 state (blue)²⁷ and E2 state (orange)²⁸, as seen from the luminal side. In the E1 state, two Ca^{2+} ions (red spheres) are coordinated by acidic and polar side chains of helices M4, M5, M6 and M8. In the E2 state, interactions of the cytoplasmic domains have caused the helices carrying these side chains to shift and rotate, which results in the disruption of the high-affinity binding site. All parts of this figure were drawn with MOLCAD in SYBYL® 6.9 Tripos Inc., 1699 South Hanley Road, St Louis, Missouri, 63144, USA.

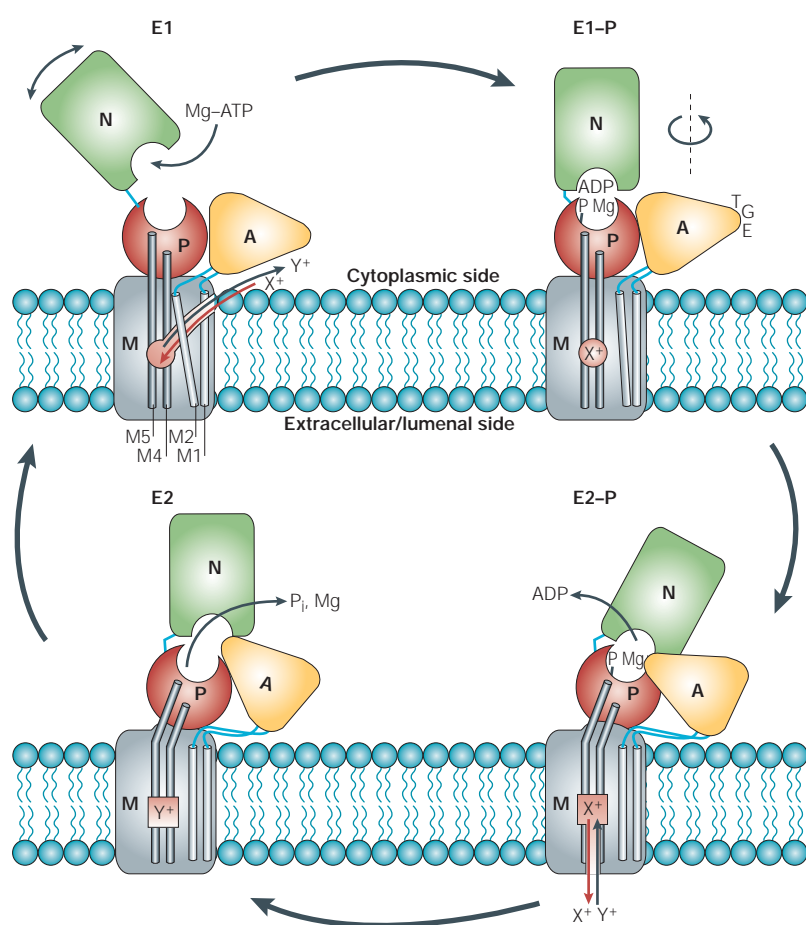


Figure 6 | Schematic diagram of the catalytic cycle of P-type ATPases. In the E1 state, ion 1 (X^+) binds to its high-affinity site in the membrane (M)-domain, which is accessible from the cytoplasm. The binding of X^+ causes the phosphorylation (P)-domain to move into the E1 conformation. As a result, the crucial Asp residue in the P-domain can be phosphorylated by Mg^{2+} -ATP, which is delivered to the phosphorylation site by the nucleotide-binding (N)-domain. In the E1-P state, the Asp is phosphorylated, but is able to transfer the phosphoryl group back to ADP. In the rate-limiting E1-P to E2-P transition, the P-domain reorientates from its E1 to its E2 position, the actuator (A)-domain rotates to bring its TGE loop into close contact with the phosphorylation site, which apparently protects the phosphoryl group against hydrolysis, and ADP dissociates. The A-domain rotation might shut off the cytoplasmic ion-access channel by a scissor movement of the attached helices M1 and M2 (light grey). Through its mechanical link to helices M4–M6 (M4 and M5 are shown in dark grey), the P-domain movement disrupts the high-affinity X^+ binding site. X^+ is released and escapes to the outside (extracellular/luminal side) through an exit channel. The ion-binding site now has a high affinity for ion 2 (Y^+), which binds from the outside. Hydrolysis of the phosphorylated Asp results in the E2 state. Mg^{2+} and inorganic phosphate (P_i) dissociate and the enzyme reverts to the E1 state, in which Y^+ is released into the cell, and another cycle begins. Mg represents Mg^{2+} throughout this figure.

and stabilizing the pentavalent transition state. In the β -PGM structure⁵³, the Mg^{2+} ion appears to protect the transition state against attack by water molecules. The Mg^{2+} ion in the phosphorylation site of P-type ATPases is likely to have a similar role.

It is interesting to note that phosphoryl transfer to the Asp proceeds only when all of the available binding sites for ion 1 are occupied³⁵, because their binding energy seems to induce the P-domain movement. Evidently, Na^+ contributes less energy than Ca^{2+} , because three Na^+ ions are required by the Na^+/K^+ -ATPase,

whereas two Ca^{2+} ions are sufficient to induce the same movement in the SR Ca^{2+} -ATPase. It therefore seems probable that the H^+ -ATPases need to bind two or three protons in this step to effect this rearrangement. As the net proton transfer is only one per ATP³², this would mean that the H^+ -ATPases counter-transport one or two protons per cycle.

Apparently, in the E1-P to E2-P transition the A-domain rotates in a plane that is roughly parallel to the membrane to bring the TGE loop close to the phosphorylation site (FIG. 6). Presumably, the resulting E2-P conformation resembles the EM-based model of the vanadate-inhibited E2-P state⁴⁸, in which the P-domain has inclined by 30°. It is possible that carboxyl and hydroxyl side chains in the TGE loop replace the phosphoryl Asp in the coordination sphere of the Mg^{2+} ion, which would then be bound to the protein even more tightly⁶⁸ (as was originally suggested by Stokes and Green, see REF. 69). The close contact of the TGE loop and the phosphorylation site in the E2-P state is corroborated by Fe^{2+} -induced cleavage experiments⁵⁹, in which Fe^{2+} in the Mg^{2+} -binding site catalyses the breakage of a peptide bond near this loop. ADP dissociates in the E1-P to E2-P transition.

The rotation of the A-domain would put a strain on M1, M2 and M3 in the M-domain, which are directly attached to it. The resulting helix movements, especially of M2 against M1, might close the polar cavity that leads from the cytoplasmic membrane surface to the ion-binding site (FIG. 6). This cavity has been proposed to be the ion-access channel in the *N. crassa* H^+ -ATPase⁵⁵ and the SR Ca^{2+} -ATPase²⁸, although there is, as yet, no evidence from mutants to support this notion²⁶.

In this assumed sequence of events, the inclination of the P-domain triggers a reversal of the helix movements that created the high-affinity sites for ion 1 in the M-domain. The coordinating side chains would reorientate, which would result in the release of ion 1 through an exit channel to the extracellular/luminal side. The new arrangement of side chains must have a high affinity for ion 2, which presumably enters through the same channel. Binding of ion 2 would then seem to stimulate hydrolysis of the phosphorylated Asp residue. Again, this might be mediated through the mechanical link of M4, M5 and M6 to the P-domain (REF. 35).

It is probable that in E2-P the bound Mg^{2+} ion competes for the hydrogen bonds of the Mg^{2+} ion, which would then no longer protect the phosphoryl Asp from attack by water. As a result, E2-P could then be hydrolysed and the Mg^{2+} ion and phosphate could subsequently escape as the TGE loop loosens its grip on the Mg^{2+} ion in the transition to the E2 state. The structure of the thapsigargin-stabilized E2 conformation²⁸ indicates that the A-domain remains roughly in place at this stage, held by molecular interactions with the N- and P-domains.

From the E2 state, the enzyme progresses to E1, in which the ion-binding site opens to the cytoplasmic side. Ion 1 then enters and pulls the helices back to their E1 position, and another cycle can start.

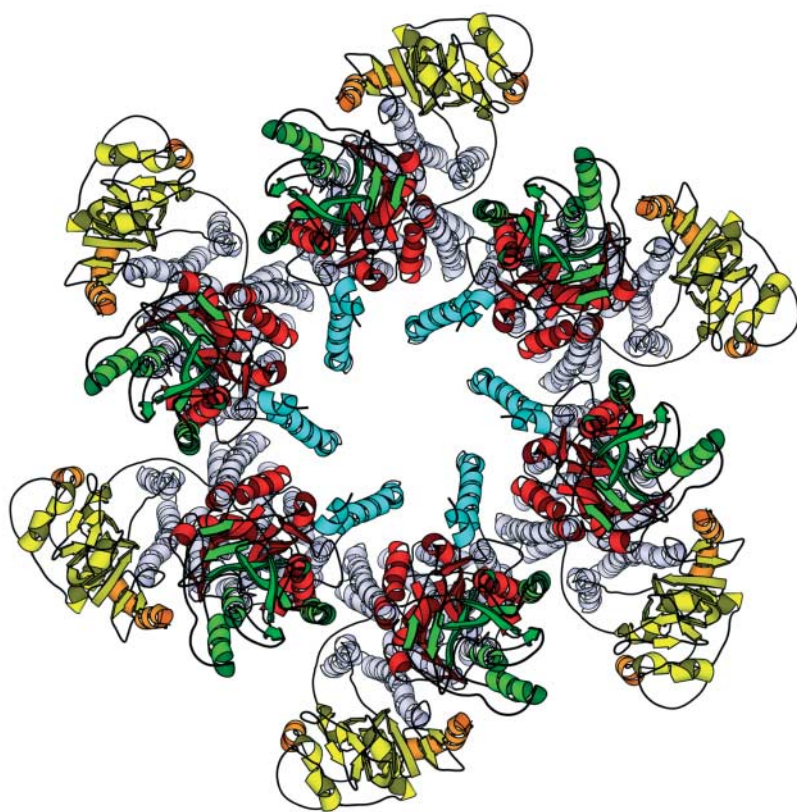


Figure 7 | Model of the *Neurospora crassa* plasma-membrane H⁺-ATPase hexamer. The figure shows a model of the *Neurospora crassa* plasma-membrane H⁺-ATPase hexamer⁵⁵ as seen from the cytoplasmic side. Hexamers form in the plasma membrane of starving *Saccharomyces cerevisiae* and *N. crassa* cells, apparently through the carboxy-terminal regulatory domains (blue), which link the nucleotide-binding domain (green) of one monomer to the phosphorylation domain (red) of an adjacent monomer. The other tight hexamer contact is between helices M3 and M10 in the membrane domain (grey). The actuator domain is shown in yellow and the amino-terminal extension is shown in orange. Reproduced with permission from REF. 55 © (2002) American Association for the Advancement of Science.

Regulation

Because of their central role in cellular metabolism, the activity of the main electrogenic P-type ATPases needs to be tightly controlled on a short enough timescale to respond to cellular and external stimuli, and stress signals. Regulation is achieved at several different levels. The amount of fungal H⁺-pump in the plasma membrane is regulated at the level of gene expression⁷⁰. The Cu⁺-transporting P-type ATPase that is affected in Menkes disease seems to be regulated at the cellular level by the redistribution of the protein from the Golgi apparatus to the plasma membrane⁷¹. The activity of the SR Ca²⁺-ATPase is modulated at the molecular level by protein–protein interactions with regulatory proteins such as phospholamban and sarcolipin (for recent reviews, see REFS 72,73). Na⁺/K⁺-ATPases and H⁺/K⁺-ATPases have regulatory β-subunits, and renal Na⁺/K⁺-ATPases have additional regulatory γ-subunits/FXYD proteins³⁵. A model of phospholamban bound to the SR Ca²⁺-ATPase⁷⁴ indicates that there are two interaction sites, one in the membrane between M2 and M9, and one in a groove on the N-domain surface. P-type ATPases of types IB, IIB and III are

14-3-3 PROTEINS

A large class of proteins that are involved in cell division, apoptosis, signal transduction, transmitter release, receptor function, gene expression and enzyme activation in eukaryotes. They function by binding to a wide range of different, specific target proteins, usually in response to phosphorylation of these targets.

regulated by domains that are fused to the main chain of the enzyme. Well-documented examples include the plasma-membrane Ca²⁺-ATPases in animals⁷⁵ and plants^{76,77}, which have amino- or carboxy-terminal calmodulin-binding regulatory domains.

The regulation of plant and fungal H⁺-pumps by the phosphorylation and dephosphorylation of autoinhibitory protein domains has been investigated in some detail. Plant H⁺-pumps have a carboxy-terminal regulatory (R)-domain of ~100 residues^{32,70,78–81}, which contains a phosphorylatable Thr residue. In its unphosphorylated state, the R-domain inactivates the H⁺-pump, probably by binding to an inhibitory site on the cytoplasmic domains. This site might correspond to a cluster of residues on the P-domain surface in the homology model for this ATPase, mutation of which results in activation³². Regulation of the plant enzyme involves 14-3-3 PROTEINS, which interact with the phosphorylated R-domain^{78,82,83} and prevent its rapid dephosphorylation. The fungal toxin fusicoccin activates the plant H⁺-pump almost irreversibly⁸⁴ by stabilizing the interaction between the phosphorylated R-domain and the 14-3-3 protein. This causes leaf stomata to open, which results in water loss and wilting that promote fungal infection. The recent X-ray structure of a 14-3-3 protein in complex with the carboxy-terminal phosphorylated pentapeptide and fusicoccin⁸⁵ showed that the last five residues of the plant R-domain are sufficient for a tight interaction.

The R-domain of fungal H⁺-pumps is only ~40 residues long, with little homology to the equivalent plant sequence. In particular, its phosphorylation site is different. Phosphorylation of Ser and/or Thr at positions –7 and –8 from the carboxyl terminus, respectively, by a specific kinase⁸⁶ activates the enzyme. An *S. cerevisiae* double mutant for these two residues locks the enzyme in an inactive state, whereas deletion of the R-domain results in constitutive activation^{70,80,87}, as it does for the plant H⁺-pump^{32,70,80}. However, regulation of the fungal pump does not involve 14-3-3 proteins. Addition of a synthetic R-domain peptide strongly activates the *N. crassa* H⁺-pump⁵⁵, whereas a corresponding peptide inhibits the plant enzyme⁷⁸. These observations indicate that the regulatory mechanism, and therefore probably the site of R-domain interaction, in fungi and plants is different.

The R-domain also seems to be responsible for the formation of H⁺-ATPase hexamers (FIG. 7). In the *N. crassa* H⁺-ATPase, the R-domain interacts with the next-door monomer through Gln624 and Arg625 (REF. 55) in helix 5 of the P-domain. This Arg residue is conserved in the fungal H⁺-ATPases that form hexamers, which highlights a role for the R-domain in oligomer formation. Low-resolution structures of isolated H⁺-ATPase hexamers in the presence and absence of Mg²⁺-ADP⁸⁸ (which is thought to induce the maximal conformational change in the active enzyme) were determined by single-particle electron cryo-microscopy⁸⁹. The largest movement, which was observed at the periphery of the cytoplasmic part of this ATPase, corresponded to the A-domain and was less than 15 Å. This movement is much smaller than the marked rearrangements that

are indicated by the EM and X-ray structures of the SR Ca^{2+} -ATPase. Therefore, either the domain movements do not need to be as extensive as the crystal structures indicate, or the H^{+} -ATPase hexamer is not fully active because these movements are restrained by tight molecular contacts (FIG. 7).

Conclusion and perspective

The high degree of structural and functional homology between the Ca^{2+} -ATPase, the $\text{Na}^{+}/\text{K}^{+}$ -ATPase and the H^{+} -ATPases indicate that they all share the same basic mechanism of ATP-driven ion translocation, which will probably apply to all P-type ATPases. The physical separation of the reactions involving ATP binding, phosphoryl transfer and hydrolysis (which occur in the three principal cytoplasmic domains) from the ion-translocation events (which occur in the membrane domain) has been preserved through evolution. Thanks to recent X-ray, EM and NMR structures of whole enzymes and individual domains, the events that accompany ATP binding and phosphoryl transfer can now be reconstructed with reasonable confidence. Likewise, on the basis of the two X-ray structures, the drastic affinity change of the ion-binding sites in the membrane can be understood in terms of the reorientation of the coordinating side chains. Nevertheless, some important aspects of the mechanism are still unclear.

The main open questions relate to the molecular events that couple the phosphorylation and dephosphorylation of the crucial Asp residue to ion transport. How exactly does the binding of ion 1 to its sites in the membrane bring about the pivotal reorientation of the P-domain to form the E1 state? Is this reorientation sufficient to induce phosphorylation? How does phosphorylation initiate the inverse movement of the P-domain, and how does this result in the release of ion 1 from the binding site in the E2-P state? It is safe

to assume that, in both processes, the energy is mechanically transmitted through M4, M5 and M6, but the exact mechanism is not clear. Other unknowns are the role of the A-domain in the dephosphorylation reaction, and how this reaction is stimulated by the binding of ion 2. Functional studies using site-directed fluorescence labelling are providing valuable new insights into the crucial transition between the E1-P and E2-P states⁹⁰, but the exact structures of these elusive intermediates are unknown.

Other questions concern the ion specificity of the various family members. This specificity must reside in the precise geometry of the side chains in the ion-binding sites, as it does in ion channels⁹¹. However, making these sites visible in sufficient detail might require structures at 2-Å resolution or higher, and it is not certain that this level of detail can be achieved with such large, inherently flexible membrane proteins. Although the basic molecular mechanism is probably the same in all P-type ion pumps, there are bound to be differences in detail. Understanding these differences will require high-resolution structures of other family members, in particular, of a $\text{Na}^{+}/\text{K}^{+}$ -ATPase, an H^{+} -ATPase, and a soft-transition-metal ATPase. Finally, there are many open questions that relate to the structural basis of regulation.

More than four decades of research on P-type ATPases have culminated in the first high-resolution X-ray structures of a family prototype — the SR Ca^{2+} -ATPase. The impact of these structures is comparable to that of the first structure of a photosynthetic reaction centre on photosynthesis research^{92,93} and the structures of bacterial K^{+} channels^{91,94,95} on molecular neurobiology research, which highlights the fundamental importance of membrane-protein structures in molecular cell biology. No doubt more structures of P-type ATPases at increasing resolution will follow to provide us with a complete picture of these fascinating molecular machines.

- Skou, J. C. The influence of some cations on an adenosine triphosphatase from peripheral nerves. *Biochim. Biophys. Acta* **23**, 394–401 (1957).
- The first description of an ATP-driven ion pump, which is now known as the $\text{Na}^{+}/\text{K}^{+}$ -ATPase. A paper worth a Nobel prize 40 years later.**
- Hasselbach, W. & Makinose, M. Die Calciumpumpe der Erschlaffungsgrana des Muskels und ihre Abhängigkeit von der ATP-Spaltung. *Eur. J. Biochem.* **333**, 518–528 (1961).
- Slayman, C. L., Lu, C. Y. & Shane, L. Correlated changes in membrane potential and ATP concentrations in *Neurospora*. *Nature* **226**, 274–276 (1970).
- Jorgensen, P. L. Purification and characterization of ($\text{Na}^{+}, \text{K}^{+}$)-ATPase V. Conformational changes in the enzyme. Transitions between the Na-form and the K-form studied with tryptic digestion as a tool. *Biochim. Biophys. Acta* **401**, 399–415 (1975).
- Jencks, W. P. Utilization of binding energy and coupling rules for active transport and other coupled vectorial processes. *Methods Enzymol.* **171**, 145–164 (1989).
- Møller, J. V., Juul, B. & le Maire, M. Structural organization, ion transport, and energy transduction of P-type ATPases. *Biochim. Biophys. Acta* **1**, 1–51 (1996).
- Axelsson, K. B. & Palmgren, M. G. Evolution of substrate specificities in the P-type ATPase superfamily. *J. Mol. Evol.* **46**, 84–101 (1998).
- A thorough analysis of the sequence homology among P-type ATPases.**
- Bull, C. J. *et al.* Complete genome sequence of the methanogenic archaeon, *Methanococcus jannaschii*. *Science* **273**, 1058–1073 (1996).
- Goffeau, A. The inventory of all ion and drug ATPases encoded by the yeast genome. *Acta Physiol. Scand.* **643**, 297–300 (1998).
- Axelsson, K. B. & Palmgren, M. G. Inventory of the superfamily of P-type ion pumps in *Arabidopsis*. *Plant Physiol.* **126**, 696–706 (2001).
- Okamura, H., Yasuhara, J. C., Fambrough, D. M. & Takeyasu, K. P-type ATPases in *Caenorhabditis* and *Drosophila*: implications for evolution of the P-type ATPase subunit families with special references to the Na,K-ATPase and H,K-ATPase subgroup. *J. Membr. Biol.* **191**, 13–24 (2002).
- Palmgren, M. G. & Axelsson, K. B. Evolution of P-type ATPases. *Biochim. Biophys. Acta* **1365**, 37–45 (1998).
- Altendorf, K. *et al.* Structure and function of the Kdp-ATPase of *Escherichia coli*. *Acta Physiol. Scand.* **643**, 137–146 (1998).
- Rensing, C., Fan, B., Sharma, R., Mitra, B. & Rosen, B. P. CopA: an *Escherichia coli* Cu(I)-translocating P-type ATPase. *Proc. Natl. Acad. Sci. USA* **97**, 652–656 (2000).
- Okkeri, J. & Haltia, T. Expression and mutagenesis of ZntA, a zinc-transporting P-type ATPase from *Escherichia coli*. *Biochemistry* **38**, 14109–14116 (1999).
- Rosen, B. P. Transport and detoxification systems for transition metals, heavy metals and metalloids in eukaryotic and prokaryotic microbes. *Comp. Biochem. Physiol., Part A Mol. Integr. Physiol.* **133**, 689–693 (2002).
- Nelson, N. Metal ion transporters and homeostasis. *EMBO J.* **18**, 4361–4371 (1999).
- Lutsenko, S. & Petris, M. J. Function and regulation of the mammalian copper-transporting ATPases: insights from biochemical and cell biological approaches. *J. Membr. Biol.* **191**, 1–12 (2003).
- Tanzi, R. E. *et al.* The Wilson disease gene is a copper transporting ATPase with homology to the Menkes disease gene. *Nature Genet.* **5**, 344–350 (1993).
- Odermatt, A., Suter, H., Krapf, R. & Solioz, M. Primary structure of two P-type ATPases involved in copper homeostasis in *Enterococcus hirae*. *J. Biol. Chem.* **268**, 12775–12779 (1993).
- Bull, P. C., Thomas, G. R., Rommens, J. M., Forbes, J. R. & Cox, D. W. The Wilson disease gene is a putative copper transporting P-type ATPase similar to the Menkes gene. *Nature Genet.* **5**, 327–337 (1993).
- Daleke, D. L. Regulation of transbilayer plasma membrane phospholipid asymmetry. *J. Lipid Res.* **44**, 233–242 (2003).
- Pomorski, T. *et al.* Drs2p-related-type ATPases Dnf1p and Dnf2p are required for phospholipid translocation across the yeast plasma membrane and serve a role in endocytosis. *Mol. Biol. Cell* **14**, 1240–1254 (2003).
- Daleke, D. L. & Huestis, W. H. Erythrocyte morphology reflects the transbilayer distribution of incorporated phospholipids. *J. Cell Biol.* **108**, 1375–1385 (1989).
- Lee, A. G. A calcium pump made visible. *Curr. Opin. Struct. Biol.* **12**, 547–554 (2002).
- Stokes, D. L. & Green, N. M. Structure and function of the calcium pump. *Annu. Rev. Biophys. Biomol. Struct.* **32**, 445–468 (2003).

- A clear and authoritative review on the SR Ca²⁺-ATPase, which puts a large amount of data into context and proposes a structure-based mechanism for the catalytic cycle.**
27. Toyoshima, C., Nakasako, M., Nomura, H. & Ogawa, H. Crystal structure of the calcium pump of sarcoplasmic reticulum at 2.6 Å resolution. *Nature* **405**, 647–655 (2000). **The first X-ray structure of a P-type ATPase defines the four principal domains, and highlights a surprisingly long distance between the ion-translocation site in the membrane and the cytoplasmic phosphorylation site.**
28. Toyoshima, C. & Nomura, H. Structural changes in the calcium pump accompanying the dissociation of calcium. *Nature* **418**, 605–611 (2002). **The 3.1-Å X-ray structure of SR Ca²⁺-ATPase trapped in an E2 state indicates significant rigid-body movements of the three cytoplasmic domains, as well as helix movements in the membrane that result in the disruption of the ion-binding site and Ca²⁺ release to the outside medium.**
29. Yu, X., Carroll, S., Rigaud, J. L. & Inesi, G. H⁺ countertransport and electrogenicity of the sarcoplasmic reticulum Ca²⁺ pump in reconstituted proteoliposomes. *Biochem. J.* **64**, 1232–1242 (1993).
30. Ma, J. J. & Pan, Z. Junctional membrane structure and store operated calcium entry in muscle cells. *Front. Biosci.* **8**, D242–D255 (2003).
31. Harper, J. F. Dissecting calcium oscillators in plant cells. *Trends Plant Sci.* **6**, 395–397 (2001).
32. Palmgren, M. G. Plant plasma membrane H⁺-ATPases: powerhouses for nutrient uptake. *Annu. Rev. Plant Physiol. Mol. Biol.* **52**, 817–845 (2001). **All there is to know about the plant proton pump — an excellent, comprehensive review.**
33. Geisler, M., Koenen, W., Richter, J. & Schumann, J. Molecular aspects of higher plant P-type Ca²⁺-ATPases. *Biochim. Biophys. Acta* **1456**, 52–78 (2000).
34. Kaplan, J. H. Biochemistry of Na,K-ATPase. *Annu. Rev. Biochem.* **71**, 511–535 (2002).
35. Jorgensen, P., Hakansson, K. & Karlsh, S. Structure and mechanism of Na,K-ATPase: functional sites and their interactions. *Annu. Rev. Physiol.* **65**, 817–849 (2003). **A detailed, authoritative review of the Na⁺/K⁺-ATPase, which puts a large body of biochemical and biophysical data into a structural context.**
36. Mense, M., Rajendran, V., Blostein, R. & Caplan, M. J. Extracellular domains, transmembrane segments, and intracellular domains interact to determine the cation selectivity of Na,K- and gastric H,K-ATPase. *Biochemistry* **41**, 9803–9812 (2002).
37. Vagin, O., Denevich, S., Munson, K. & Sachs, G. SCH28080, a K⁺-competitive inhibitor of the gastric H,K-ATPase, binds near the M5–6 luminal loop, preventing K⁺ access to the ion binding domain. *Biochemistry* **41**, 12755–12762 (2002).
38. Monk, B. C. & Perlin, D. S. Fungal plasma membrane proton pumps as promising new antifungal targets. *Crit. Rev. Microbiol.* **20**, 209–223 (1994).
39. Besancon, M. *et al.* Membrane topology and omeprazole labeling of the gastric H⁺/K⁺-adenosinetriphosphatase. *Biochemistry* **32**, 2345–2355 (1993).
40. Geering, K. The functional role of β subunits in oligomeric P-type ATPases. *J. Bioenerg. Biomembr.* **33**, 425–438 (2001).
41. Therien, A. G., Pu, H. X., Karlsh, S. J. & Blostein, R. Molecular and functional studies of the γ subunit of the sodium pump. *J. Bioenerg. Biomembr.* **33**, 407–414 (2001).
42. Geering, K. *et al.* FXYD proteins: new tissue- and isoform-specific regulators of Na,K-ATPase. *Ann. NY Acad. Sci.* **986**, 388–394 (2003).
43. Morsomme, P. *et al.* Characterization of a hyperthermophilic P-type ATPase from *Methanococcus jannaschii* expressed in yeast. *J. Biol. Chem.* **277**, 29608–29616 (2002).
44. Eraso, P. & Gancedo, C. Activation of yeast plasma membrane ATPase by acid pH during growth. *FEBS Lett.* **224**, 187–192 (1987).
45. Skriver, E., Maunsbach, A. B. & Jorgensen, P. L. Formation of two-dimensional crystals in pure membrane-bound (Na⁺/K⁺)-ATPase. *FEBS Lett.* **131**, 219–222 (1981).
46. Dux, L. & Martonosi, A. Two-dimensional arrays of proteins in sarcoplasmic reticulum and purified Ca²⁺-ATPase vesicles treated with vanadate. *J. Biol. Chem.* **258**, 2599–2603 (1983).
47. Rabon, E., Wilke, M., Sachs, G. & Zampighi, G. Crystallization of the gastric H,K-ATPase. *J. Mol. Biol.* **261**, 1434–1439 (1986).
48. Xu, C., Rice, W. J., He, W. & Stokes, D. L. A structural model for the catalytic cycle of Ca²⁺-ATPase. *J. Mol. Biol.* **316**, 201–211 (2002). **A 6-Å map of the vanadate-inhibited SR Ca²⁺-ATPase indicates a central role for the A-domain in the catalytic cycle.**
49. Rice, W. J. *et al.* Structure of Na⁺/K⁺-ATPase at 11-Å resolution: comparison with Ca²⁺-ATPase in E1 and E2 states. *Biophys. J.* **80**, 2187–2197 (2001). **The best structure of a Na⁺/K⁺-ATPase so far highlights a close similarity to the SR Ca²⁺-ATPase in the E2-P state.**
50. Auer, M., Scarborough, G. A. & Kühlbrandt, W. Three-dimensional map of the plasma membrane H⁺-ATPase in the open conformation. *Nature* **392**, 840–843 (1998). **The first, and so far only, structure of an H⁺-pump in an E1 state, which was determined to an 8-Å resolution by electron crystallography.**
51. Jahn, T. *et al.* Large scale expression, purification and 2D crystallization of recombinant plant plasma membrane H⁺-ATPase. *J. Mol. Biol.* **309**, 465–476 (2001).
52. Zhang, P., Toyoshima, C., Yonekura, K., Green, N. M. & Stokes, D. L. Structure of the calcium pump from sarcoplasmic reticulum at 8 Å resolution. *Nature* **392**, 835–839 (1998).
53. Lahiri, S. D., Zhang, G., Dunaway-Mariano, D. & Allen, K. N. The pentavalent phosphorus intermediate of a phosphoryl transfer reaction. *Science* **299**, 2067–2071 (2003). **The 1.2-Å structure of a close homologue of the P-type-ATPase P-domain shows the crucial Asp residue in the process of being phosphorylated.**
54. Hilge, M. *et al.* ATP-induced conformational changes of the nucleotide-binding domain of Na,K-ATPase. *Nature Struct. Biol.* **10**, 468–474 (2003). **The solution NMR structure of a recombinant N-domain shows the triphosphate of ATP protruding from the nucleotide-binding pocket.**
55. Kühlbrandt, W., Zeelen, J. & Dietrich, J. Structure, mechanism, and regulation of the *Neurospora* plasma membrane H⁺-ATPase. *Science* **297**, 1692–1696 (2002). **A homology model of the *M. crassa* H⁺-pump highlights a significant difference in the position of the N-domain compared with the SR Ca²⁺-ATPase. In addition, the position of the carboxy-terminal R-domain of the H⁺-pump indicates a structure-based mechanism of enzyme regulation.**
56. Ogawa, H. & Toyoshima, C. Homology modeling of the cation binding sites of Na⁺/K⁺-ATPase. *Proc. Natl Acad. Sci. USA* **99**, 15977–15982 (2002).
57. Aravind, L., Galperin, M. Y. & Koonin, E. V. The catalytic domain of the P-type ATPase has the haloacid dehalogenase fold. *Trends Biochem. Sci.* **23**, 127–129 (1998).
58. Toyofuku, T., Kurzydowski, K., Tada, M. & MacLennan, D. H. Amino acids Lys-Asp-Asp-Lys-Pro-Val402 in the Ca(2+)-ATPase of cardiac sarcoplasmic reticulum are critical for functional association with phospholamban. *J. Biol. Chem.* **269**, 22929–22932 (1994).
59. Patchornik, G., Goldsheger, R. & Karlsh, S. J. The complex ATP-Fe²⁺ serves as a specific affinity cleavage reagent in ATP-Mg²⁺ sites of Na,K-ATPase: altered ligation of Fe²⁺ (Mg²⁺) ions accompanies the E₁P→E₂P conformational change. *Proc. Natl Acad. Sci. USA* **97**, 11954–11959 (2000).
60. Gitschier, J., Moffat, B., Reilly, D., Wood, W. I. & Fairbrother, W. J. Solution structure of the fourth metal-binding domain from the Menkes copper-transporting ATPase. *Nature Struct. Biol.* **5**, 47–54 (1998).
61. Banci, L. *et al.* A new zinc-protein coordination site in intracellular metal trafficking: solution structure of the Apo and Zn(II) forms of ZntA(46–118). *J. Mol. Biol.* **323**, 883–897 (2002).
62. Hill, E. E., Morea, V. & Chothia, C. Sequence conservation in families whose members have little or no sequence similarity: the four-helical cytokines and cytochromes. *J. Mol. Biol.* **322**, 205–233 (2002).
63. Baldwin, J. M. The probable arrangement of the helices in G protein-coupled receptors. *EMBO J.* **12**, 1693–1703 (1993).
64. Buch-Pedersen, M. J. *et al.* Abolishment of proton pumping and accumulation in the E1P conformational state of a plant plasma membrane H⁺-ATPase by substitution of a conserved aspartyl residue in transmembrane segment 6. *J. Biol. Chem.* **275**, 39167–39173 (2000).
65. Buch-Pedersen, M. J. & Palmgren, M. G. Conserved Asp684 in transmembrane segment M6 of the plant plasma membrane P-type proton pump AHA2 is a molecular determinant of proton translocation. *J. Biol. Chem.* **278**, 17845–17851 (2003).
66. Bukrinsky, J. T., Buch-Pedersen, M. J., Larsen, S. & Palmgren, M. G. A putative proton binding site of plasma membrane H⁺-ATPase identified through homology modelling. *FEBS Lett.* **494**, 6–10 (2001).
67. Danko, S., Yamasaki, K., Daiho, T., Suzuki, H. & Toyoshima, C. Organization of cytoplasmic domains of sarcoplasmic reticulum Ca²⁺-ATPase in E₁P and E₂ ATP states: a limited proteolysis study. *FEBS Lett.* **505**, 129–135 (2001).
68. Wakabayashi, S. & Shigekawa, M. Role of divalent cation bound to phosphoenzyme intermediate of sarcoplasmic reticulum ATPase. *J. Biol. Chem.* **259**, 4427–4436 (1984).
69. Stokes, D. L. & Green, N. M. Modeling a dehalogenase fold into the 8-Å density map for Ca(2+)-ATPase defines a new domain structure. *Biophys. J.* **78**, 1765–1776 (2000).
70. Portillo, F. Regulation of plasma membrane H⁺-ATPase in fungi and plants. *Biochim. Biophys. Acta* **1469**, 31–42 (2000).
71. Petris, M. J. *et al.* Ligand-regulated transport of the Menkes copper P-type ATPase efflux pump from the Golgi apparatus to the plasma membrane: a novel mechanism of regulated trafficking. *EMBO J.* **15**, 6084–6095 (1996).
72. East, J. M. Sarcoplasmic reticulum calcium pumps: recent advances in our understanding of structure/function and biology. *Mol. Membr. Biol.* **17**, 189–200 (2000).
73. MacLennan, D. H. & Kranias, E. G. Phospholamban: a crucial regulator of cardiac contractility. *Nature Rev. Mol. Cell Biol.* **4**, 566–577 (2003).
74. Toyoshima, C. *et al.* Modeling of the inhibitory interaction of phospholamban with the Ca²⁺ ATPase. *Proc. Natl Acad. Sci. USA* **100**, 467–472 (2003).
75. Carafoli, E. Biogenesis: plasma membrane calcium ATPase: 15 years of work on the purified enzyme. *FASEB J.* **8**, 993–1002 (1994).
76. Curran, A. C. *et al.* Autoinhibition of a calmodulin-dependent calcium pump involves a structure in the stalk that connects the transmembrane domain to the ATPase catalytic domain. *J. Biol. Chem.* **275**, 30301–30308 (2000).
77. Sze, H., Liang, F., Hwang, I., Curran, A. C. & Harper, J. F. Diversity and regulation of plant Ca²⁺ pumps: insights from expression in yeast. *Annu. Rev. Plant Physiol. Mol. Biol.* **51**, 433–462 (2000).
78. Palmgren, M. G., Sommarin, M., Serrano, R. & Larsson, C. Identification of an autoinhibitory domain in the C-terminal region of the plant plasma membrane H⁺-ATPase. *J. Biol. Chem.* **266**, 20470–20475 (1991).
79. Palmgren, M. Regulation of plant plasma-membrane H⁺-ATPase activity. *Physiol. Plantarum* **83**, 314–323 (1991).
80. Serrano, R., Portillo, F., Monk, B. C. & Palmgren, M. G. The regulatory domain of fungal and plant plasma membrane H⁺-ATPase. *Acta Physiol. Scand. Suppl.* **607**, 131–136 (1992).
81. Morsomme, P., Slayman, C. W. & Goffeau, A. Mutagenic study of the structure, function and biogenesis of the yeast plasma membrane H⁺-ATPase. *Biochim. Biophys. Acta* **1469**, 133–157 (2000).
82. Oecking, C., Piotrowski, M., Hagemeyer, J. & Hagemann, K. Topology of the fusicoccin-binding 14-3-3 homologs of *Commelina communis*. *Plant J.* **12**, 441–453 (1997).
83. Fuglsang, A. T. *et al.* Binding of 14-3-3 protein to the plasma membrane H⁺-ATPase AHA2 involves the three C-terminal residues Tyr(946)-Thr(Val) and requires phosphorylation of Thr(947). *J. Biol. Chem.* **274**, 36774–36780 (1999).
84. Aducci, P., Marra, M., Fogliano, V. & Fullone, M. R. Fusicoccin receptors: perception and transduction of the fusicoccin-signal. *J. Exp. Bot.* **46**, 1463–1478 (1995).
85. Würtele, M., Jelich-Ottmann, C., Wittinghofer, A. & Oecking, C. Structural view of a fungal toxin acting on a 14-3-3 regulatory complex. *EMBO J.* **22**, 987–994 (2003). **An X-ray structure of a complex of the last five residues of the plant H⁺-ATPase R-domain with a 14-3-3 protein shows how a fungal toxin activates this proton pump.**
86. Goossens, A., de la Fuente, N., Forment, J., Serrano, R. & Portillo, F. Regulation of yeast H⁺-ATPase by protein kinases belonging to a family dedicated to activation of plasma membrane transporters. *Mol. Cell. Biol.* **20**, 7654–7661 (2000).
87. Portillo, F., Eraso, P. & Serrano, R. Analysis of the regulatory domain of yeast plasma membrane H⁺-ATPase by directed mutagenesis and intragenic suppression. *FEBS Lett.* **287**, 71–74 (1991).
88. Goormaghtigh, E., Vigneron, L., Scarborough, G. A. & Ruyschaert, J. M. Tertiary conformational changes of the *Neurospora crassa* plasma membrane H⁺-ATPase monitored by hydrogen/deuterium exchange kinetics. A Fourier transformed infrared spectroscopy approach. *J. Biol. Chem.* **269**, 27409–27413 (1994).
89. Rhee, K. H., Scarborough, G. A. & Henderson, R. Domain movements of plasma membrane H⁺-ATPase: 3D structures of two states by electron cryo-microscopy. *EMBO J.* **21**, 3582–3589 (2002).
90. Geibel, S., Kaplan, J. H., Bamberg, E. & Freidrich, T. Conformational dynamics of the Na⁺/K⁺-ATPase probed by voltage clamp fluorometry. *Proc. Natl Acad. Sci. USA* **100**, 964–969 (2003).

91. Zhou, Y., Morais-Cabral, J. H., Kaufman, A. & MacKinnon, R. Chemistry of ion coordination and hydration revealed by a K⁺ channel-Fab complex at 2.0 Å resolution. *Nature* **414**, 43–48 (2001).
92. Deisenhofer, J. & Michel, H. The photosynthetic reaction centre from the purple bacterium *Rhodospseudomonas viridis*. *Biosci. Rep.* **9**, 383–419 (1989).
93. Rhee, K. H. Photosystem II: the solid structural era. *Annu. Rev. Biophys. Biomol. Struct.* **30**, 307–328 (2001).
94. Doyle, D. A. *et al.* The structure of the potassium channel: molecular basis of K⁺ conduction and selectivity. *Science* **280**, 69–77 (1998).
95. Jiang, Y. *et al.* X-ray structure of a voltage-dependent K⁺ channel. *Nature* **423**, 33–41 (2003).
96. Albers, R. Biochemical aspects of active transport. *Annu. Rev. Biochem.* **36**, 727–756 (1967).
97. Post, R. L., Hegyvary, C. & Kume, S. Activation by adenosine triphosphate in the phosphorylation kinetics of sodium and potassium ion transport adenosine triphosphatase. *J. Biol. Chem.* **247**, 6530–6540 (1972).
98. Henderson, R. *et al.* Model for the structure of bacteriorhodopsin based on high-resolution electron cryo-microscopy. *J. Mol. Biol.* **213**, 899–929 (1990).
99. Kühlbrandt, W., Wang, D. N. & Fujiyoshi, Y. Atomic model of plant light-harvesting complex by electron crystallography. *Nature* **367**, 614–621 (1994).
100. Miyazawa, A., Fujiyoshi, Y. & Unwin, N. Structure and gating mechanism of the acetylcholine receptor pore. *Nature* **423**, 949–955 (2003).
101. Chothia, C. & Lesk, A. M. The relation between the divergence of sequence and structure in proteins. *EMBO J.* **5**, 823–826 (1986).
102. Altschul, S. F. *et al.* Gapped BLAST and PSI-BLAST: a new generation of protein database search programs. *Nucleic Acids Res.* **25**, 3389–3402 (1997).
103. Thompson, J. D., Higgins, D. G. & Gibson, T. J. CLUSTAL W: improving the sensitivity of progressive multiple sequence alignment through sequence weighting, position-specific gap penalties and weight matrix choice. *Nucleic Acids Res.* **22**, 4673–4680 (1994).
104. Sali, A. & Blundell, T. L. Comparative protein modelling by satisfaction of spatial restraints. *J. Mol. Biol.* **234**, 779–815 (1993).

Acknowledgements

I thank Gitte Mohsin and Paolo Lastrico for preparing the figures, and Mickey Palmgren for many helpful hints.

Competing interests statement

The author declares that he has no competing financial interests.

Online links

DATABASES

The following terms in this article are linked online to:

Entrez: <http://www.ncbi.nlm.nih.gov/entrez/>

CadA | CopA | KdpA | KdpB | KdpC | KdpF | ZntA

Protein Data Bank: <http://www.rcsb.org/pdb/>

Ca²⁺-ATPase, E1 state | Ca²⁺-ATPase, E2 state | H⁺-ATPase

Access to this interactive links box is free online.